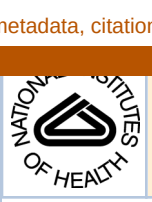

Published in final edited form as:

Cytoskeleton (Hoboken). 2012 August ; 69(8): 577–590. doi:10.1002/cm.21035.

Computer-assisted image analysis of human cilia and *Chlamydomonas* flagella reveals both similarities and differences in axoneme structure

Eileen T. O'Toole[1], **Thomas H. Giddings Jr.**[2], **Mary E. Porter**[3,†], and **Lawrence E. Ostrowski**[4,†,*]

[1]Boulder Laboratory for 3D Electron Microscopy of Cells, Dept. MCD Biology, University of Colorado, Boulder, CO 80309-347

[2]Dept. MCD Biology, University of Colorado, Boulder, CO 80309-347

[3]Dept. of Genetics, Cell Biology and Development, University of Minnesota, Minneapolis, MN 55455

[4]Dept. of Pulmonary and Critical Care Medicine, University of North Carolina, Chapel Hill, NC 27599

Abstract

In the past decade, investigations from several different fields have revealed the critical role of cilia in human health and disease. Because of the highly conserved nature of the basic axonemal structure, many different model systems have proven useful for the study of ciliopathies, especially the unicellular, biflagellate green alga, *Chlamydomonas reinhardtii*. Although the basic axonemal structure of cilia and flagella is highly conserved, these organelles often perform specialized functions unique to the cell or tissue in which they are found. These differences in function are likely reflected in differences in structural organization. In this work, we directly compare the structure of isolated axonemes from human cilia and *Chlamydomonas* flagella to identify similarities and differences that potentially play key roles in determining their functionality. Using transmission electron microscopy and 2D image averaging techniques, our analysis has confirmed the overall structural similarity between these two species, but also revealed clear differences in the structure of the outer dynein arms, the central pair projections, and the radial spokes. We also show how the application of 2D image averaging can clarify the underlying structural defects associated primary ciliary dyskinesia (PCD). Overall, our results document the remarkable similarity between these two structures separated evolutionarily by over a billion years, while highlighting several significant differences, and demonstrate the potential of 2D image averaging to improve the diagnosis and understanding of PCD.

Keywords

dynein; image averaging; primary ciliary dyskinesia

[*]Correspondence to: Lawrence E. Ostrowski, Ph.D., The University of North Carolina at Chapel Hill, School of Medicine, Cystic Fibrosis/Pulmonary Research and Treatment Center, Dept of Cell and Developmental Biology, CB# 7248, 6123A Thurston-Bowles Bldg. Chapel Hill, NC 27599-7248, Voice: (919) 843-7177, FAX: (919) 966-5178, ostro@med.unc.edu.

[†]These two authors contributed equally to this work.

[±]A portion of this work was previously presented at the Microscopy and Microanalysis Meeting (2008) held in Albuquerque, NM.

Introduction

Cilia and flagella are complex organelles that can serve as both sensory structures and contribute to cell motility. Primary cilia, or nonmotile cilia, can be found on nearly every cell in the human body; they perform principally a sensory function. Motile cilia and flagella are found on diverse cell types and are responsible for a variety of movements ranging from the swimming of single cells to the transport of fluids over specialized epithelia (Silflow and Lefebvre 2001; Vincensini et al. 2011). For example, sperm cells use a single flagellum for propulsion, while ciliated cells in the ventricles of the brain use hundreds of coordinated cilia to drive the circulation of cerebrospinal fluid. Most motile cilia and flagella are built upon a common structure, the 9+2 axoneme constructed from nine outer doublet microtubules, a central pair of microtubules with associated projections, and two rows of dynein arms that serve as the molecular motors for motility. However, although there is a high degree of structural conservation between e.g., a sperm flagellum and an ependymal cilium, it is clear that these structures have evolved to perform specific functions in these different cell types.

Defects in the structure and function of cilia have recently been shown to result in a wide spectrum of human diseases. "Ciliopathy" is the allinclusive term used to describe any disease that can be caused by defects in cilia structure or function. These diseases range from autosomal dominant polycystic kidney disease, caused by mutations in polycystin-1 or polycystin-2, that localize to the primary cilium of renal epithelial cells, to primary ciliary dyskinesia (PCD), in which defects in the motile cilia in the airways cause repeated pulmonary infections (Badano et al. 2006; Fliegauf et al. 2007; Ostrowski et al. 2011). PCD is a genetically heterogeneous disease in which biallelic mutations cause a defect in one of the many proteins required for the assembly and function of cilia (Bush et al. 2007; Kennedy and Ostrowski 2006; Leigh et al. 2009a; Noone et al. 2004; Zariwala et al. 2011). This defect results in impaired or absent mucociliary clearance, and leads to sinusitis, otitis media, chronic airways infection, and bronchiectasis that in some cases is so severe a lung transplant is the only available treatment option. PCD is difficult to diagnose, and it is likely that some people with PCD are not identified and consequently, do not receive proper treatment (Leigh et al. 2011; Leigh et al. 2009b; Olin et al. 2011; Wodehouse et al. 2003). The current method for diagnosing PCD relies on a compatible clinical phenotype and subjective evaluation of transmission electron micrographs of cross sections of cilia to identify defects in the axonemal structure (i.e., missing inner and/or outer dynein arms).

Because of the highly conserved nature of ciliary structure, many different organisms have been useful to investigate the pathogenesis of ciliopathies (Badano et al. 2006; Fliegauf et al. 2007; Hildebrandt et al. 2011; Ostrowski et al. 2011). In particular, the unicellular alga, *Chlamydomonas*, has been a useful model organism to study PCD. Biochemical, molecular and structural approaches have been used to identify a large number of mutations in *Chlamydomonas* that affect the assembly or function of specific axonemal structures including those that affect the inner and outer dynein arms, the central pair microtubules, and the radial spokes (as reviewed in (Porter and Sale 2000)). Comparative genomic and proteomic studies have shown that the axoneme contains ~600 proteins, many of which are highly conserved (Avidor-Reiss et al. 2004; Li et al. 2004; Ostrowski et al. 2002; Pazour et al. 2005). To date, only about ~200 of the proteins have been correlated with a specific structure, and most of that work has been done using *Chlamydomonas* as a model system. These studies have shown that very small defects in axoneme structure can have profound effects on motility. The first PCD causing mutations were identified in a dynein intermediate chain gene, *DNAI1*, using a candidate gene approach based on similar structural abnormalities observed in mutant strains of *Chlamydomonas* and PCD patients (Pennarun et al. 1999).

Even though the basic structure of human ciliary and *Chlamydomonas* flagellar axonemes are extensively conserved, there are functional differences between these organelles. For example, the 12 um *Chlamydomonas* flagella can beat with two different waveforms at frequencies of up 60 Hz, enabling propulsion in opposite directions, while human respiratory cilia are approximately 7 um long and beat with a single waveform at much lower frequencies (10-15 Hz) to transport mucus out of the airways (Silflow and Lefebvre 2001; Wanner et al. 1996). Further, the regulation of axonemal activity is very different between these two species. For example, an increase in cAMP stimulates ciliary beat frequency in human cilia, while causing a decrease in *Chlamydomonas* (Wanner et al. 1996). Similarly, an increase in Ca++ stimulates ciliary beat frequency in human cilia, while causing *Chlamydomonas* flagella to change from an asymmetric waveform to a symmetric waveform (Silflow and Lefebvre 2001; Wanner et al. 1996). It is likely that these functional differences are also reflected in structural differences between these two axonemes. However, even though advanced techniques for imaging biological structures have been applied to the analysis of simple biological systems, e.g., flagella from *Chlamydomonas* (Mastronarde et al. 1992; Nicastro et al. 2011; Nicastro et al. 2005; O'Toole et al. 1995; Sui and Downing 2006) these same procedures have not yet been applied to human cilia, in part because of the limited availability of material. Advances in the methods used to culture human airway epithelial cells (Fulcher et al. 2005; Gray et al. 1996) and the development of methods to reproducibly isolate human cilia have now made these studies possible (Ostrowski 2006).

Here, we describe the application of a 2D image averaging technique to analyze isolated human ciliary axonemes to determine the structure of this important organelle in greater detail. Recently, several elegant studies using cryoelectron tomography have revealed organization of the dynein arms, radial spokes, and central pair complexes in a number of organisms at unprecedented resolution (Bui et al. 2011; Hoog et al. 2012; Pigino et al. 2011). However, while cryoelectron tomography has significantly improved resolution and provided new information, it is extremely time consuming and expensive, and it has not yet been applied to human material. The combination of standard thin section EM and 2D image averaging is a more accessible, lower cost alternative method that could be more readily applied to better define the structure of human ciliary axonemes, and can be used to confirm/complement the results of other studies. We show here how this approach can provide new insights into the organization of human cilia and identify both similarities and differences between human cilia and *Chlamydomonas* flagella. We also demonstrate how 2D image averaging can be used to clarify structural defects in cilia from a PCD patient. These studies suggest that 2D image averaging could be a useful tool in the diagnosis of more subtle PCD mutations and also lay the groundwork for future studies using higher resolution approaches.

Results and Discussion

Overall structural similarity of the human ciliary and *Chlamydomonas* flagellar axoneme

The goal of this study was to directly compare the structure of the axoneme from human respiratory cilia with the axoneme from *Chlamydomonas* flagella. We have previously used transmission electron microscopy and image averaging techniques to understand the diversity and organization of dynein arms and other structures in *Chlamydomonas* (reviewed in (Porter and Sale 2000)). Image averaging procedures improve the signal-to-noise ratio to better visualize repeating elements of axonemal structure. Further, the programs allow statistical comparisons between axonemes from wild-type and mutant samples. Ciliary axonemes were isolated from well-differentiated cultures of human airway epithelial cells in the presence of a detergent to remove the membrane and soluble matrix components for improved resolution of the axonemal structure (Kultgen et al. 2002; Ostrowski 2006). Flagella were isolated from wild-type *Chlamydomonas* cells by pH shock and

demembranated with detergent as previously described (Porter et al. 1992). Both preparations were processed in parallel for electron microscopy with the identical fixative solution (2% glutaraldehyde / 4% tannic acid) to improve contrast and eliminate fixationinduced differences between the samples.

Routine cross-sections obtained by transmission electron microscopy (TEM) demonstrated the expected overall similarity between these two structures, including the nine outer microtubule doublets surrounding the central pair microtubule complex (Figure 1 A, B). As previously reported, *Chlamydomonas* flagella have several unique structures located in the proximal portion of the axoneme that have not been observed in the human axoneme; these include the bridge structure between doublets 1 and 2 and the Btubule projections ("beak") in doublets 1, 5, and 6 (Hoops and Witman 1983) (*not shown*). In addition, *Chlamydomonas* lacks an outer dynein arm on outer doublet microtubule 1 (Figure 1A;*). Thus although the overall similarity of the two axoneme preparations is apparent, structural differences are also present that likely reflect differences in function.

Comparison of human and *Chlamydomonas* outer doublet cross-sections

To compare the structure of the human and *Chlamydomonas* axonemes in greater detail, we employed the technique of 2-D image averaging (Mastronarde et al. 1992; O'Toole et al. 1995). While this procedure has been useful for examining axoneme organization in *Chlamydomonas*, and similar procedures have been applied to human axonemes (e.g., (Carson et al. 2000; Escudier et al. 2002)), to our knowledge, a direct comparison between axonemes from these two species has not been performed. For this study, images of isolated axonemes in cross section were digitized and averaged as detailed in Methods. Increasing the number of images included in the average increases the signal-to-noise in order to resolve the individual protofilaments that comprise the microtubule doublets and the attached inner and outer dynein arm structures. Doublets that contained protofilaments visible in cross section were selected, rotated into a common orientation, aligned and averaged. The resulting averages from *Chlamydomonas* (Figure 1C) and from human cilia (Figure 1D) show remarkable similarities. However, comparisons between the two sets of averages revealed a major difference in the structure of the outer dynein arm with *Chlamydomonas* having an extra region of density on the ODA not present in the human (Figure 1 C, D; arrow). This difference can be explained by the fact that, while the *Chlamydomonas* outer dynein arm is a three-headed structure containing three dynein heavy chains (α, β, γ), the human outer dynein arm is believed to be a two-headed structure containing two dynein heavy chains. This is based partly on the lack of a human homologue of the α heavy chain (Pazour et al. 2006) and evidence from other mammalian species of a two-headed outer dynein arm (Hastie et al. 1988; Hom et al. 2011; Nicastro et al. 2006; Pazour et al. 2006). The presence of a third dynein heavy chain is a common feature of outer arm dyneins in protists (Wickstead and Gull 2007). *Chlamydomonas* mutants lacking the α dynein heavy chain show reduced motility and beat frequency *in vivo* (Sakakibara et al. 1991), while *in vitro*, isolated outer dynein arms lacking the α subunit showed increased ATPase activity but reduced microtubule gliding (Furuta et al. 2009). Interestingly, in *Chlamydomonas,* the outer dynein arms are identical along the length of the axoneme, whereas in human cilia, the composition of the outer arm dynein heavy chains varies between the proximal and distal regions (Fliegauf et al. 2005). Thus while the overall structure and organization of the outer dynein arms is remarkably similar between human cilia and *Chlamydomonas* flagella, there exist distinct structural differences that are clearly a reflection of the differences in the underlying molecular composition of outer arm dynein complexes (reviewed in (Hom et al. 2011)).

Comparison of human and *Chlamydomonas* central pair structures

Defects in the structure of the central pair complex have also been shown to affect the motility of cilia and flagella (reviewed in Mitchell, (Mitchell 2004; Mitchell and Smith 2009)). Several central pair mutations and polypeptides have been identified in *Chlamydomonas* ((Adams et al. 1981; Dutcher et al. 1984), reviewed in Mitchell, (Mitchell and Smith 2009)), but less is known about the organization of the central pair microtubules in human cilia. Figure 2A shows an average of the *Chlamydomonas* central pair complex. As reported previously (Goodenough and Heuser 1985; Mitchell and Smith 2009), the C1 and C2 microtubules are connected by a bipartite bridge and a diagonal link (Figure 2B; b, dl, respectively). Each central pair microtubule is associated with a distinct set of projections that repeat in a characteristic fashion along its length (Figure 2A, B).

To obtain comparable images of the central pair microtubules and projections from human cilia, profiles of axonemes from human cilia were digitized in a standard orientation with dynein arms pointing clockwise and an imaginary line drawn through the central pair that would intersect doublet number one on the top and bisect doublets 5 and 6 on the bottom. A model point was then placed between the CP microtubules and complexes from multiple axonemes were extracted, aligned and averaged. Interestingly, the positions of the nine radial spokes are enhanced in the human average because the central pair does not rotate within the axoneme as it does in *Chlamydomonas* (Silflow and Lefebvre 2001). As shown in Figures 2C and 2D, the CP microtubules in human cilia are also connected by a bipartite bridge and diagonal linker. In addition, many of the projections associated with each central pair microtubule in *Chlamydomonas* appear to be conserved in human axonemes, with projection domains that vary slightly in length and/or shape (Figure 2D). Most notably, the projections from the C2 microtubule appear enhanced in the human axoneme compared to the *Chlamydomonas* axoneme, much like that reported for the CP projections in mouse (Lechtreck et al. 2008), while the C1a projection of *Chlamydomonas* is enhanced compared to human (Figure 2; *). However, some of the central pair projections appear different between the two species with an additional density detected adjacent to the C1c domain in human (Figure 2D; *).

Analyses of mutations in *Chlamydomonas* that disrupt the assembly of specific projections have identified discrete subsets of axonemal polypeptides associated with each projection (reviewed in Mitchell, (Mitchell and Smith 2009)). As shown in Table 1, many of these have human orthologues that show a high degree of identity/similarity with the *Chlamydomonas* protein. For example, SPAG6 is 65% identical with 82% sequence coverage to PF16 and has been identified in human cilia by proteomic analysis (Ostrowski et al. 2002). Hydin is 44% identical with 87% sequence coverage, and mutations in hydin cause hydrocephalus in mice (Lechtreck et al. 2008). Similarly, Pcdp1 is 38% identical with 50% sequence coverage to FAP221, and deletion of this C1d projection protein causes PCD in mice (Lee et al. 2008). In contrast, FAP46 is only 28% identical with 7% sequence coverage to C10orf93, and FAP54 is only 30% identical with 13% sequence coverage with C12orf55. Thus the structural similarities and differences in the central pair are reflected in the presence of both conserved and unique proteins.

Comparison of inner dynein arms and radial spokes between human cilia and *Chlamydomonas* flagella

To compare the structural organization of the inner dynein arms and the radial spokes, we averaged longitudinal sections of both *Chlamydomonas* and human axonemes. In *Chlamydomonas*, the outer row of dynein arms repeat every 24 nm but the inner arm region is more complex, consisting of at least ten densities that repeat every 96 nm along the length of the microtubule when viewed by thin section TEM and 2D image averaging (Porter and

Sale 2000). The complexity of inner arm organization is revealed as one compares the raw images to the averages of individual axonemes, and then compares the individual averages from many axonemes to grand averages from multiple samples (Figure 3). Longitudinal sections of human cilia that have clearly visible outer dynein arms and a central pair microtubule were chosen for analysis (Figure 3 A). Several images of the 96 nm repeats were selected by placing a model point in the center of the 96 nm repeat (Figure 3A; black dots), and averages were obtained along individual axonemes (Figure 3B;). Averages from separate axonemes were then aligned to each other and averaged to obtain a grand average from many axonemes (Figure 3C; average contains 13 axonemes, total of 120 repeats) and from multiple individuals (Figure 3D; grand average contains total of 25 axonemes, 223 repeats).

We have previously used 2D averaging to characterize several different mutations in *Chlamydomonas* that affect the assembly of various inner arm isoforms as well as the dynein regulatory complex (DRC) located above the second radial spoke (Gardner et al. 1994; Mastronarde et al. 1992; Porter and Sale 2000; Rupp and Porter 2003). As several of the dynein polypeptides associated with these structures have been identified in both *Chlamydomonas* and humans (Hom et al. 2011), we were interested in determining how well these structures might be conserved in human axonemes. Comparing the averages obtained from the longitudinal images of *Chlamydomonas* flagella (Figure 4A) with the average obtained from human cilia (Figure 4B) reveals a remarkable degree of similarity in the organization of the inner dynein arms. This can be seen more clearly in the difference map between the two averages (Figure 4C). For example, the trilobed I1 dynein located proximal to the first radial spoke is clearly present in both images, as well as the smaller single-headed dynein isoforms located at discrete positions within the 96 nm repeat(Gardner et al. 1994; Mastronarde et al. 1992; Porter and Sale 2000). However, some of the densities present in *Chlamydomonas* axonemes appear different in human ciliary axonemes. For example, human cilia have a reduced density in one of the lobes above RS3, and an additional density between S3 and S1. These differences may reflect the greater complexity of inner arm isoforms necessary to produce different waveforms (Hom et al. 2011; Porter et al. 1996).

Slight differences in density are also apparent in the region associated with the dynein regulatory complex (Figure 4D; DRC) (Gardner et al. 1994; Mastronarde et al. 1992; Rupp and Porter 2003). In particular, the density of the dynein regulatory complex appears to be slightly increased in *Chlamydomonas* relative to the human axoneme, with an increased density adjacent to the DRC in human cilia. CryoET has recently demonstrated that the DRC is part of the extended nexin link (N-DRC) that connects the adjacent outer doublet microtubules (Heuser et al. 2009). The thin section images shown here only include a portion of the N-DRC; further imaging of human axonemes using cryoET will be required to understand the organization of this structure at higher resolution and in three dimensions. Additional work is also needed to determine how the subunit composition of the DRC might vary between these two species.

In contrast with the conserved structure of the inner dynein arms, human axonemes contain a third radial spoke that is clearly seen in the difference map (Figure 4C), and a slightly reduced density in the head region of radial spoke 1The presence of a third radial spoke is common in most other species, and has been previously examined in detail, for example, in mussel gill cilia and rat sperm flagella (Olson and Linck 1977; Warner and Satir 1974). Recent cryoET studies have demonstrated that while radial spoke 1 and 2 in *Chlamydomonas* are very similar, the third radial spoke in *Tetrahymena* and *Strongylocentrotus* is unique (Barber et al. 2012; Lin et al. 2012; Pigino et al. 2011). The human average also shows that the third radial spoke is different in shape with a wider spoke

head and a faint diagonal linker compared with spokes 1 and 2 (Figures 4B, D). Because the majority of molecular and biochemical investigations of radial spokes have used *Chlamydomonas*, it is not known if the third radial spoke contains unique proteins, or if its unique structure represents a different organization of proteins present in radial spokes 1 and 2. Table 2 lists the known radial spoke proteins of *Chlamydomonas* and the closest human orthologue. Interestingly, *Chlamydomonas* has been shown to contain a short structure (known as the radial spoke stand-in) that localizes to the position of the third radial spoke (Barber et al. 2012; Lin et al. 2012; Pigino et al. 2011). This structure corresponds to the base of the third radial spoke in human cilia, as only the spoke head is observed in the difference map (Figure 4C).

Application of 2D image averaging to analyze structural defects in PCD

To demonstrate the usefulness of 2D image averaging to resolve potential inner arm defects associated with PCD, which are difficult to resolve by standard TEM (Escudier et al. 2002; O'Callaghan et al. 2011), we also generated averages of human ciliary axonemes from cells isolated from a patient previously diagnosed as missing inner dynein arms, in particular, DHC7 (Zhang et al. 2002). Comparing the image averages between controls (Figure 5A) and the patient (Figure 5B) clearly demonstrates the absence of the inner dynein arms in this patient. As a disease control, we also processed cilia isolated from human airway epithelial cells cultured from a cystic fibrosis (CF) patient in parallel. As expected, cilia from the CF cells demonstrated an intact inner arm structure (Figure 5C). Examining longitudinal sections from the PCD cilia further demonstrates the almost complete absence of inner dynein arms, including the I1 dynein, indicating that the mutation in this patient disrupts the assembly of most, if not all, inner dynein arms. This is consistent with genetic studies that have identified mutations in CCDC39 in this patient (unpublished observation, M. Knowles and M. Zariwala). CCDC39 is the human orthologue of *Chlamydomonas* FAP59, and has been reported to be essential for the formation of inner dynein arms and the dynein regulatory complex, and mutations in CCDC39 have been shown to cause PCD (Merveille et al. 2011). CCDC39 mutations have also been reported to result in significant axonemal disorganization (mislocalized peripheral doublets with displacement or absence of the central pair). It has been difficult to determine if these latter effects are secondary consequences of the defects in inner arm assembly or reflect a role for CCDC39 in the organization of the outer doublets. The results shown here, although obtained from selected images, suggest that CCDC39 is critical for the assembly of the inner dynein arms and portions of the DRC, but may not be absolutely required for axoneme integrity.

Conclusion

While several studies have examined the structure of human cilia by conventional EM, the use of advanced image analysis techniques to examine the structure of human cilia in detail has not been previously reported. In an effort to improve the diagnosis of PCD, two prior studies took advantage of the radial symmetry of axonemes to average the outer doublets (Carson et al. 2000; Escudier et al. 2002). While this procedure improved the resolution of the inner and outer dynein arms, it completely obscured the central pair. Similarly, Afzelius et al. applied the technique of image averaging to cross-sections of sperm from normal individuals and to a patient with PCD and demonstrated the absence of dynein arms in the PCD patient (Afzelius et al. 1995). In this work, we have used 2D image analysis programs developed in our lab to study the axonemal structure of human cilia and compare the results with those obtained from *Chlamydomonas* flagella. Overall, these structures are remarkably conserved. However, averages from human axonemes show distinct differences in structure that likely reflect the differences in motility of these two organelles. Major differences include the presence of a two-headed outer dynein arm and three radial spokes in human

cilia, consistent with previous work on metazoan cilia. The central pair complex in human also contains C2 projections that are larger relative to those seen in *Chlamydomonas*, and an additional density located adjacent to the C1c domain. Longitudinal averages revealed that the overall arrangement of inner dynein arms within the 96 nm axoneme repeat is remarkably similar, but some inner arm structures as well as portions of the DRC in human axonemes appear to be reduced in density and differ slightly from *Chlamydomonas* in size and shape. It should be pointed out that while image averaging techniques improve the resolution of regularly repeated structures, these same procedures will average out structures that occur irregularly. For example, structures that are only present in the proximal or distal region of the axoneme may not appear in the averaged image. Further detailed studies will be required to fully define the structure of human cilia.

We also applied 2D image averaging to compare the organization of the inner dynein arms in normal patients with that observed in a PCD patient and a CF disease control. Averages from cross sections and longitudinal views suggest that the assembly of most of the inner dynein arms is significantly disrupted in the PCD patient compared with both the normal human average and the disease control. Difference images confirm that most of the inner arm dyneins and a portion of the DRC are not assembled in the PCD patient. In summary, this work has documented similarities and differences between the structure of the axoneme from human cilia and *Chlamydomonas* flagella. The approach described here should also be useful in the diagnosis and further studies of PCD, particularly those cases with more subtle structural defects.

Materials and Methods

Preparation of Chlamydomonas flagella

Wild-type *Chlamydomonas reinhardtii* were cultured as previously described and flagella were isolated using the pH-shock procedure (Porter et al. 1992). *Chlamydomonas* axonemes were extracted with 0.1% NP-40 and prepared for electron microscopy by fixation in 2% glutaraldehyde, 4% tannic acid (Porter et al. 1992).

Preparation of human cilia

Human airway epithelial cells obtained from lung transplant or donor tissues under protocols approved by the University of North Carolina Institutional Review Board were cultured at an air/liquid interface on collagen coated membranes using established techniques (Fulcher et al. 2005; Gray et al. 1996). After the cultures had differentiated into a wellciliated epithelium, ciliary axonemes were isolated using a buffer containing 0.1% Triton X-100 and 10 mM calcium (Ostrowski 2006) and fixed in the identical fixative solution used for the *Chlamydomonas* flagella (above). Cilia from two control (not CF; not PCD) donors were used for the comparison to *Chlamydomonas* and the longitudinal average. Cilia from a different control donor were used for the comparison to the individual PCD and CF samples in cross-section.

Electron Microscopy and Image Analysis

Fixed samples of *Chlamydomonas* flagella and human cilia were postfixed in 1% OsO4, embedded in Epon-Araldite, and processed for TEM using standard procedures (Porter et al. 1992).

Negatives were scanned using a Microtek ScanMaker i900 at a pixel size of 1 nm and the digital images were analyzed using programs in the IMOD software package developed in the Boulder 3D lab (Mastronarde et al. 1992; O'Toole et al. 1995). These programs are freely available to download (http://bio3d.colorado.edu/imod). Briefly, 60nm sections were

used for cross section analysis. Images of axonemes containing outer doublets in cross section were chosen for analysis if they had a complete set of 9 outer doublet microtubules, an intact central pair and protofilaments that were visible in at least one outer doublet microtubule. Approximately 50-100 outer doublets were selected for a given sample. The individual outer doublets were extracted, rotated into approximate alignment, aligned by applying a general linear transformation, and averaged to obtain a sample average. The doublet sample average for *Chlamydomonas* contained 140 doublets. The doublet average for the normal human contained 110 doublets. The doublet average for the PCD and CF patient contained 132 and 109 doublets, respectively. Averages of CP complexes from *Chlamydomonas* were obtained by digitizing axonemes in standard orientation as described (Mitchell and Smith 2009). Central pair complexes from human cilia were obtained with axonemes oriented with doublet number one in the 12 o'clock position. A total of 45 CP complexes and 46 CP complexes were used for the *Chlamydomonas* and human averages, respectively. Longitudinal averages were computed from 40nm thin sections containing profiles of axonemes that contain two outer doublets separated by the central pair microtubules. Individual 96 nm inner arm repeats were extracted and aligned to obtain a sample average. Axoneme averages were then aligned to obtain the grand average. A total 10 axonemes (82 repeats), 25 axonemes (223 repeats) and 8 axonemes (65 repeats) were used to compute the longitudinal average for *Chlamydomonas,* normal human and PCD patient, respectively. Difference images were computed using an ANOVA at each pixel with differences not significant to 0.0025 confidence level set to zero.

Acknowledgments

We wish to thank Amanda Bednarz, R. Wonsetler, and K. Burns for technical support and electron microscopy. This work was supported by National Institutes of Health (NIH) grant GM55667 to MEP and Cystic Fibrosis Foundation grant R026. The Boulder Laboratory for 3D EM of Cells is supported by NIH grant RR-00592 to Andreas Hoenger.

References

Adams GM, Huang B, Piperno G, Luck DJ. Centralpair microtubular complex of Chlamydomonas flagella: polypeptide composition as revealed by analysis of mutants. J Cell Biol. 1981; 91(1):69–76. [PubMed: 7028763]

Afzelius BA, Dallai R, Lanzavecchia S, Bellon PL. Flagellar structure in normal human spermatozoa and in spermatozoa that lack dynein arms. Tissue Cell. 1995; 27(3):241–7. [PubMed: 7645004]

Avidor-Reiss T, Maer AM, Koundakjian E, Polyanovsky A, Keil T, Subramaniam S, Zuker CS. Decoding cilia function: defining specialized genes required for compartmentalized cilia biogenesis. Cell. 2004; 117(4):527–39. [PubMed: 15137945]

Badano JL, Mitsuma N, Beales PL, Katsanis N. The Ciliopathies: An Emerging Class of Human Genetic Disorders. Annu Rev Genomics Hum Genet. 2006

Barber CF, Heuser T, Carbajal-Gonzalez BI, Botchkarev VV Jr. Nicastro D. Three-dimensional structure of the radial spokes reveals heterogeneity and interactions with dyneins in Chlamydomonas flagella. Mol Biol Cell. 2012; 23(1):111–20. [PubMed: 22072792]

Bui KH, Pigino G, Ishikawa T. Three-dimensional structural analysis of eukaryotic flagella/cilia by electron cryotomography. J Synchrotron Radiat. 2011; 18(1):2–5. [PubMed: 21169680]

Bush A, Chodhari R, Collins N, Copeland F, Hall P, Harcourt J, Hariri M, Hogg C, Lucas J, Mitchison HM. Primary ciliary dyskinesia: current state of the art. Arch Dis Child. 2007; 92(12):1136–40. others. [PubMed: 17634184]

Carson JL, Hu SS, Collier AM. Computer-assisted analysis of radial symmetry in human airway epithelial cilia: assessment of congenital ciliary defects in primary ciliary dyskinesia. Ultrastruct Pathol. 2000; 24(3):169–74. [PubMed: 10914428]

Dutcher SK, Huang B, Luck DJ. Genetic dissection of the central pair microtubules of the flagella of Chlamydomonas reinhardtii. J Cell Biol. 1984; 98(1):229–36. [PubMed: 6707088]

Escudier E, Couprie M, Duriez B, Roudot-Thoraval F, Millepied MC, Pruliere-Escabasse V, Labatte L, Coste A. Computer-assisted analysis helps detect inner dynein arm abnormalities. Am J Respir Crit Care Med. 2002; 166(9):1257–62. [PubMed: 12403696]

Fliegauf M, Benzing T, Omran H. When cilia go bad: cilia defects and ciliopathies. Nat Rev Mol Cell Biol. 2007; 8(11):880–93. [PubMed: 17955020]

Fliegauf M, Olbrich H, Horvath J, Wildhaber JH, Zariwala MA, Kennedy M, Knowles MR, Omran H. Mislocalization of DNAH5 and DNAH9 in respiratory cells from patients with primary ciliary dyskinesia. American Journal of Respiratory and Critical Care Medicine. 2005; 171(12):1343–1349. [PubMed: 15750039]

Fulcher ML, Gabriel S, Burns KA, Yankaskas JR, Randell SH. Well-differentiated human airway epithelial cell cultures. Methods Mol Med. 2005; 107:183–206. [PubMed: 15492373]

Furuta A, Yagi T, Yanagisawa HA, Higuchi H, Kamiya R. Systematic comparison of in vitro motile properties between Chlamydomonas wild-type and mutant outer arm dyneins each lacking one of the three heavy chains. J Biol Chem. 2009; 284(9):5927–35. [PubMed: 19124458]

Gardner LC, O'Toole E, Perrone CA, Giddings T, Porter ME. Components of a "dynein regulatory complex" are located at the junction between the radial spokes and the dynein arms in Chlamydomonas flagella. J Cell Biol. 1994; 127(5):1311–25. [PubMed: 7962092]

Goodenough UW, Heuser JE. Substructure of inner dynein arms, radial spokes, and the central pair/projection complex of cilia and flagella. J Cell Biol. 1985; 100(6):2008–18. [PubMed: 2860115]

Gray TE, Guzman K, Davis CW, Abdullah LH, Nettesheim P. Mucociliary differentiation of serially passaged normal human tracheobronchial epithelial cells. Am. J. Respir. Cell Mol. Biol. 1996; 14:104–112. [PubMed: 8534481]

Hastie AT, Marchese-Ragona SP, Johnson KA, Wall JS. Structure and mass of mammalian respiratory ciliary outer arm 19S dynein. Cell Motil Cytoskeleton. 1988; 11(3):157–66. [PubMed: 2974760]

Heuser T, Raytchev M, Krell J, Porter ME, Nicastro D. The dynein regulatory complex is the nexin link and a major regulatory node in cilia and flagella. J Cell Biol. 2009; 187(6):921–33. [PubMed: 20008568]

Hildebrandt F, Benzing T, Katsanis N. Ciliopathies. N Engl J Med. 2011; 364(16):1533–43. [PubMed: 21506742]

Hom EF, Witman GB, Harris EH, Dutcher SK, Kamiya R, Mitchell DR, Pazour GJ, Porter ME, Sale WS, Wirschell M. A unified taxonomy for ciliary dyneins. Cytoskeleton (Hoboken). 2011; 68(10):555–65. others. [PubMed: 21953912]

Hoog JL, Bouchet-Marquis C, McIntosh JR, Hoenger A, Gull K. Cryoelectron tomography and 3-D analysis of the intact flagellum in Trypanosoma brucei. J Struct Biol. 2012

Hoops HJ, Witman GB. Outer doublet heterogeneity reveals structural polarity related to beat direction in Chlamydomonas flagella. J Cell Biol. 1983; 97(3):902–8. [PubMed: 6224802]

Kennedy MP, Ostrowski LE. Primary ciliary dyskinesia and upper airway diseases. Curr Allergy Asthma Rep. 2006; 6(6):513–7. [PubMed: 17026878]

Kultgen PL, Byrd SK, Ostrowski LE, Milgram SL. Characterization of an akinase anchoring protein in human ciliary axonemes. Mol Biol Cell. 2002; 13(12):4156–66. [PubMed: 12475942]

Lechtreck KF, Delmotte P, Robinson ML, Sanderson MJ, Witman GB. Mutations in Hydin impair ciliary motility in mice. J Cell Biol. 2008; 180(3):633–43. [PubMed: 18250199]

Lee L, Campagna DR, Pinkus JL, Mulhern H, Wyatt TA, Sisson JH, Pavlik JA, Pinkus GS, Fleming MD. Primary ciliary dyskinesia in mice lacking the novel ciliary protein Pcdp1. Mol Cell Biol. 2008; 28(3):949–57. [PubMed: 18039845]

Leigh MW, O'Callaghan C, Knowles MR. The challenges of diagnosing primary ciliary dyskinesia. Proc Am Thorac Soc. 2011; 8(5):434–7. [PubMed: 21926395]

Leigh MW, Pittman JE, Carson JL, Ferkol TW, Dell SD, Davis SD, Knowles MR, Zariwala MA. Clinical and genetic aspects of primary ciliary dyskinesia/Kartagener syndrome. Genet Med. 2009a; 11(7):473–87. [PubMed: 19606528]

citLeigh MW, Zariwala MA, Knowles MR. Primary ciliary dyskinesia: improving the diagnostic approach. Curr Opin Pediatr. 2009b; 21(3):320–5.

Li JB, Gerdes JM, Haycraft CJ, Fan Y, Teslovich TM, May-Simera H, Li H, Blacque OE, Li L, Leitch CC. Comparative genomics identifies a flagellar and basal body proteome that includes the BBS5 human disease gene. Cell. 2004; 117(4):541–52. others. [PubMed: 15137946]

Lin J, Heuser T, Carbajal-Gonzalez BI, Song K, Nicastro D. The Structural Heterogeneity of Radial Spokes in Cilia and Flagella is Conserved. Cytoskeleton (Hoboken). 2012; 69:88–100. [PubMed: 22170736]

Mastronarde DN, O'Toole ET, McDonald KL, McIntosh JR, Porter ME. Arrangement of inner dynein arms in wild-type and mutant flagella of Chlamydomonas. J Cell Biol. 1992; 118(5):1145–62. [PubMed: 1387403]

Merveille AC, Davis EE, Becker-Heck A, Legendre M, Amirav I, Bataille G, Belmont J, Beydon N, Billen F, Clement A. CCDC39 is required for assembly of inner dynein arms and the dynein regulatory complex and for normal ciliary motility in humans and dogs. Nat Genet. 2011; 43(1): 72–8. others. [PubMed: 21131972]

Mitchell DR. Speculations on the evolution of 9+2 organelles and the role of central pair microtubules. Biol Cell. 2004; 96(9):691–6. [PubMed: 15567523]

Mitchell DR, Smith B. Analysis of the central pair microtubule complex in Chlamydomonas reinhardtii. Methods Cell Biol. 2009; 92:197–213. [PubMed: 20409807]

Nicastro D, Fu X, Heuser T, Tso A, Porter ME, Linck RW. Cryoelectron tomography reveals conserved features of doublet microtubules in flagella. Proc Natl Acad Sci U S A. 2011; 108(42):E845–53. [PubMed: 21930914]

Nicastro D, McIntosh JR, Baumeister W. 3D structure of eukaryotic flagella in a quiescent state revealed by cryoelectron tomography. Proc Natl Acad Sci U S A. 2005; 102(44):15889–94. [PubMed: 16246999]

Nicastro D, Schwartz C, Pierson J, Gaudette R, Porter ME, McIntosh JR. The molecular architecture of axonemes revealed by cryoelectron tomography. Science. 2006; 313(5789):944–8. [PubMed: 16917055]

Noone PG, Leigh MW, Sannuti A, Minnix SL, Carson JL, Hazucha M, Zariwala MA, Knowles MR. Primary ciliary dyskinesia: diagnostic and phenotypic features. Am J Respir Crit Care Med. 2004; 169(4):459–67. [PubMed: 14656747]

O'Callaghan C, Rutman A, Williams GM, Hirst RA. Inner dynein arm defects causing primary ciliary dyskinesia: repeat testing required. Eur Respir J. 2011; 38(3):603–7. [PubMed: 21406509]

O'Toole E, Mastronarde D, McIntosh JR, Porter ME. Computer-assisted analysis of flagellar structure. Methods Cell Biol. 1995; 47:183–91. [PubMed: 7476486]

Olin JT, Burns K, Carson JL, Metjian H, Atkinson JJ, Davis SD, Dell SD, Ferkol TW, Milla CE, Olivier KN. Diagnostic yield of nasal scrape biopsies in primary ciliary dyskinesia: A multicenter experience. Pediatr Pulmonol. 2011 others.

Olson GE, Linck RW. Observations of the structural components of flagellar axonemes and central pair microtubules from rat sperm. J Ultrastruct Res. 1977; 61(1):21–43. [PubMed: 915974]

Ostrowski, L. Preparation of cilia from human airway epithelial cells. In: Celis, J., editor. Cell Biology: A Laboratory Handbook. Elsevier Science; San Diego: 2006. p. 99-102.

Ostrowski LE, Blackburn K, Radde KM, Moyer MB, Schlatzer DM, Moseley A, Boucher RC. A proteomic analysis of human cilia: identification of novel components. Mol Cell Proteomics. 2002; 1(6):451–65. [PubMed: 12169685]

Ostrowski LE, Dutcher SK, Lo CW. Cilia and models for studying structure and function. Proc Am Thorac Soc. 2011; 8(5):423–9. [PubMed: 21926393]

Pazour GJ, Agrin N, Leszyk J, Witman GB. Proteomic analysis of a eukaryotic cilium. J Cell Biol. 2005; 170(1):103–13. [PubMed: 15998802]

Pazour GJ, Agrin N, Walker BL, Witman GB. Identification of predicted human outer dynein arm genes: candidates for primary ciliary dyskinesia genes. J Med Genet. 2006; 43(1):62–73. [PubMed: 15937072]

Pennarun G, Escudier E, Chapelin C, Bridoux AM, Cacheux V, Roger G, Clement A, Goossens M, Amselem S, Duriez B. Loss-of-function mutations in a human gene related to Chlamydomonas reinhardtii dynein IC78 result in primary ciliary dyskinesia. Am J Hum Genet. 1999; 65(6):1508–19. [PubMed: 10577904]

Pigino G, Bui KH, Maheshwari A, Lupetti P, Diener D, Ishikawa T. Cryoelectron tomography of radial spokes in cilia and flagella. J Cell Biol. 2011; 195(4):673–87. [PubMed: 22065640]

Porter ME, Knott JA, Myster SH, Farlow SJ. The dynein gene family in Chlamydomonas reinhardtii. Genetics. 1996; 144(2):569–85. [PubMed: 8889521]

Porter ME, Power J, Dutcher SK. Extragenic suppressors of paralyzed flagellar mutations in Chlamydomonas reinhardtii identify loci that alter the inner dynein arms. J Cell Biol. 1992; 118(5):1163–76. [PubMed: 1387404]

Porter ME, Sale WS. The 9 + 2 axoneme anchors multiple inner arm dyneins and a network of kinases and phosphatases that control motility. J Cell Biol. 2000; 151(5):F37–42. [PubMed: 11086017]

Rupp G, Porter ME. A subunit of the dynein regulatory complex in Chlamydomonas is a homologue of a growth arrestspecific gene product. J Cell Biol. 2003; 162(1):47–57. [PubMed: 12847082]

Sakakibara H, Mitchell DR, Kamiya R. A Chlamydomonas outer arm dynein mutant missing the alpha heavy chain. J Cell Biol. 1991; 113(3):615–22. [PubMed: 1673127]

Silflow CD, Lefebvre PA. Assembly and motility of eukaryotic cilia and flagella. Lessons from Chlamydomonas reinhardtii. Plant Physiol. 2001; 127(4):1500–7. [PubMed: 11743094]

Sui H, Downing KH. Molecular architecture of axonemal microtubule doublets revealed by cryoelectron tomography. Nature. 2006; 442(7101):475–8. [PubMed: 16738547]

Vincensini L, Blisnick T, Bastin P. 1001 model organisms to study cilia and flagella. Biol Cell. 2011; 103(3):109–30. [PubMed: 21275904]

Wanner A, Salathe M, O'Riordan TG. Mucociliary clearance in the airways. Am. J. Respir. Crit. Care Med. 1996; 154:1868–1902. [PubMed: 8970383]

Warner FD, Satir P. The structural basis of ciliary bend formation. Radial spoke positional changes accompanying microtubule sliding. J Cell Biol. 1974; 63(1):35–63. [PubMed: 4424314]

Wickstead B, Gull K. Dyneins across eukaryotes: a comparative genomic analysis. Traffic. 2007; 8(12):1708–21. [PubMed: 17897317]

Wodehouse T, Kharitonov SA, Mackay IS, Barnes PJ, Wilson R, Cole PJ. Nasal nitric oxide measurements for the screening of primary ciliary dyskinesia. Eur Respir J. 2003; 21(1):43–7. [PubMed: 12570107]

Zariwala MA, Omran H, Ferkol TW. The emerging genetics of primary ciliary dyskinesia. Proc Am Thorac Soc. 2011; 8(5):430–3. [PubMed: 21926394]

Zhang YJ, O'Neal WK, Randell SH, Blackburn K, Moyer MB, Boucher RC, Ostrowski LE. Identification of dynein heavy chain 7 as an inner arm component of human cilia that is synthesized but not assembled in a case of primary ciliary dyskinesia. J Biol Chem. 2002; 277(20): 17906–15. [PubMed: 11877439]

1. Dutcher SK, Huang B, Luck DJ. Genetic dissection of the central pair microtubules of the flagella of Chlamydomonas reinhardtii. J Cell Biol. 1984; 98(1):229–36. PMCID: 2113000. [PubMed: 6707088]

2. Smith EF, Lefebvre PA. PF16 encodes a protein with armadillo repeats and localizes to a single microtubule of the central apparatus in Chlamydomonas flagella. J Cell Biol. 1996; 132(3):359–70. PMCID: 2120723. [PubMed: 8636214]

3. Neilson LI, Schneider PA, Van Deerlin PG, Kiriakidou M, Driscoll DA, Pellegrini MC, et al. cDNA cloning and characterization of a human sperm antigen (SPAG6) with homology to the product of the Chlamydomonas PF16 locus. Genomics. 1999; 60(3):272–80. [PubMed: 10493827]

4. Yang P, Fox L, Colbran RJ, Sale WS. Protein phosphatases PP1 and PP2A are located in distinct positions in the Chlamydomonas flagellar axoneme. J Cell Sci. 2000; 113(Pt 1):91–102. [PubMed: 10591628]

5. Han Y, Haines CJ, Feng HL. Role(s) of the serine/threonine protein phosphatase 1 on mammalian sperm motility. Arch Androl. 2007; 53(4):169–77. [PubMed: 17852041]

6. Rupp G, O'Toole E, Porter ME. The Chlamydomonas PF6 locus encodes a large alanine/proline-rich polypeptide that is required for assembly of a central pair projection and regulates flagellar motility. Mol Biol Cell. 2001; 12(3):739–51. PMCID: 30977. [PubMed: 11251084]

7. Wargo MJ, Dymek EE, Smith EF. Calmodulin and PF6 are components of a complex that localizes to the C1 microtubule of the flagellar central apparatus. J Cell Sci. 2005; 118(Pt 20):4655–65. [PubMed: 16188941]

8. Zhang Z, Jones BH, Tang W, Moss SB, Wei Z, Ho C, et al. Dissecting the axoneme interactome: the mammalian orthologue of Chlamydomonas PF6 interacts with sperm-associated antigen 6, the mammalian orthologue of Chlamydomonas PF16. Mol Cell Proteomics. 2005; 4(7):914–23. [PubMed: 15827353]

9. Zhang H, Mitchell DR. Cpc1, a Chlamydomonas central pair protein with an adenylate kinase domain. J Cell Sci. 2004; 117(Pt 18):4179–88. PMCID: 1525021. [PubMed: 15292403]

10. Mitchell BF, Pedersen LB, Feely M, Rosenbaum JL, Mitchell DR. ATP production in Chlamydomonas reinhardtii flagella by glycolytic enzymes. Mol Biol Cell. 2005; 16(10):4509–18. PMCID: 1237060. [PubMed: 16030251]

11. Ostrowski LE, Andrews K, Potdar P, Matsuura H, Jetten A, Nettesheim P. Cloning and characterization of KPL2, a novel gene induced during ciliogenesis of tracheal epithelial cells. Am J Respir Cell Mol Biol. 1999; 20:675–83. [PubMed: 10100999]

12. Sironen A, Thomsen B, Andersson M, Ahola V, Vilkki J. An intronic insertion in KPL2 results in aberrant splicing and causes the immotile short-tail sperm defect in the pig. Proc Natl Acad Sci U S A. 2006; 103(13):5006–11. PMCID: 1458785. [PubMed: 16549801]

13. Bloch MA, Johnson KA. Identification of a molecular chaperone in the eukaryotic flagellum and its localization to the site of microtubule assembly. J Cell Sci. 1995; 108(Pt 11):3541–5. [PubMed: 8586665]

14. DiPetrillo CG, Smith EF. Pcdp1 is a central apparatus protein that binds Ca(2+)-calmodulin and regulates ciliary motility. J Cell Biol. 2010; 189(3):601–12. PMCID: 2867295. [PubMed: 20421426]

15. Lee L, Campagna DR, Pinkus JL, Mulhern H, Wyatt TA, Sisson JH, et al. Primary ciliary dyskinesia in mice lacking the novel ciliary protein Pcdp1. Mol Cell Biol. 2008; 28(3):949–57. [PubMed: 18039845]

16. Lechtreck KF, Witman GB. Chlamydomonas reinhardtii hydin is a central pair protein required for flagellar motility. J Cell Biol. 2007; 176(4):473–82. [PubMed: 17296796]

17. Davy BE, Robinson ML. Congenital hydrocephalus in hy3 mice is caused by a frameshift mutation in Hydin, a large novel gene. Hum Mol Genet. 2003; 12(10):1163–70. [PubMed: 12719380]

18. Bernstein M, Beech PL, Katz SG, Rosenbaum JL. A new kinesin-like protein (Klp1) localized to a single microtubule of the Chlamydomonas flagellum. J Cell Biol. 1994; 125(6):1313–26. PMCID: 2290928. [PubMed: 8207060]

19. Yokoyama R, O'Toole E, Ghosh S, Mitchell DR. Regulation of flagellar dynein activity by a central pair kinesin. Proc Natl Acad Sci U S A. 2004; 101(50):17398–403. PMCID: 536025. [PubMed: 15572440]

20. Smith EF, Lefebvre PA. PF20 gene product contains WD repeats and localizes to the intermicrotubule bridges in Chlamydomonas flagella. Mol Biol Cell. 1997; 8(3):455–67. PMCID: 276097. [PubMed: 9188098]

21. Pennarun G, Bridoux AM, Escudier E, Dastot-Le Moal F, Cacheux V, Amselem S, et al. Isolation and expression of the human hPF20 gene orthologous to Chlamydomonas PF20: evaluation as a candidate for axonemal defects of respiratory cilia and sperm flagella. Am J Respir Cell Mol Biol. 2002; 26(3):362–70. [PubMed: 11867345]

22. Zhang Z, Zariwala MA, Mahadevan MM, Caballero-Campo P, Shen X, Escudier E, et al. A heterozygous mutation disrupting the SPAG16 gene results in biochemical instability of central apparatus components of the human sperm axoneme. Biol Reprod. 2007; 77(5):864–71. [PubMed: 17699735]

23. Mitchell, DR. The Flagellar Central Pair Apparatus. In: Harris, EH., editor. The Chlamydomonas Sourcebook: Introduction to Chlamydomonas and Its Laboratory Use: Elsevier Science. 2009. p. 235-52.

1. Yang P, Diener DR, Yang C, Kohno T, Pazour GJ, Dienes JM, et al. Radial spoke proteins of Chlamydomonas flagella. J Cell Sci. 2006; 119(Pt 6):1165–74. PMCID: 1973137. [PubMed: 16507594]

2. Shetty J, Klotz KL, Wolkowicz MJ, Flickinger CJ, Herr JC. Radial spoke protein 44 (human meichroacidin) is an axonemal alloantigen of sperm and cilia. Gene. 2007; 396(1):93–107. PMCID: 1935023. [PubMed: 17451891]

3. Yang P, Yang C, Sale WS. Flagellar radial spoke protein 2 is a calmodulin binding protein required for motility in Chlamydomonas reinhardtii. Eukaryot Cell. 2004; 3(1):72–81. PMCID: 329519. [PubMed: 14871938]
4. Williams BD, Velleca MA, Curry AM, Rosenbaum JL. Molecular cloning and sequence analysis of the Chlamydomonas gene coding for radial spoke protein 3: flagellar mutation pf-14 is an ochre allele. J Cell Biol. 1989; 109(1):235–45. [PubMed: 2745550]
5. Curry AM, Williams BD, Rosenbaum JL. Sequence analysis reveals homology between two proteins of the flagellar radial spoke. Mol Cell Biol. 1992; 12(9):3967–77. [PubMed: 1508197]
6. Castleman VH, Romio L, Chodhari R, Hirst RA, de Castro SC, Parker KA, et al. Mutations in radial spoke head protein genes RSPH9 and RSPH4A cause primary ciliary dyskinesia with central-microtubular-pair abnormalities. Am J Hum Genet. 2009; 84(2):197–209. PMCID: 2668031. [PubMed: 19200523]
7. Fiedler SE, Sisson JH, Wyatt TA, Pavlik JA, Gambling TM, Carson JL, et al. Loss of ASP but not ROPN1 reduces mammalian ciliary motility. Cytoskeleton (Hoboken). 2012; 69(1):22–32. PMCID: 3261315. [PubMed: 22021175]
8. Merchant SS, Prochnik SE, Vallon O, Harris EH, Karpowicz SJ, Witman GB, et al. The Chlamydomonas genome reveals the evolution of key animal and plant functions. Science. 2007; 318(5848):245–50. PMCID: 2875087. [PubMed: 17932292]
9. Yang C, Compton MM, Yang P. Dimeric novel HSP40 is incorporated into the radial spoke complex during the assembly process in flagella. Mol Biol Cell. 2005; 16(2):637–48. PMCID: 545900. [PubMed: 15563613]
10. Guan J, Ekwurtzel E, Kvist U, Hultenby K, Yuan L. DNAJB13 is a radial spoke protein of mouse '9+2' axoneme. Reprod Domest Anim. 2010; 45(6):992–6. [PubMed: 19919626]
11. Yang P, Diener DR, Rosenbaum JL, Sale WS. Localization of calmodulin and dynein light chain LC8 in flagellar radial spokes. J Cell Biol. 2001; 153(6):1315–26. PMCID: 2192029. [PubMed: 11402073]
12. King SM, Patel-King RS. The M(r) = 8,000 and 11,000 outer arm dynein light chains from Chlamydomonas flagella have cytoplasmic homologues. J Biol Chem. 1995; 270(19):11445–52. [PubMed: 7744782]
13. Yang P, Yang C, Wirschell M, Davis S. Novel LC8 mutations have disparate effects on the assembly and stability of flagellar complexes. J Biol Chem. 2009; 284(45):31412–21. PMCID: 2781537. [PubMed: 19696030]
14. Patel-King RS, Gorbatyuk O, Takebe S, King SM. Flagellar radial spokes contain a Ca2+-stimulated nucleoside diphosphate kinase. Mol Biol Cell. 2004; 15(8):3891–902. PMCID: 491844. [PubMed: 15194815]
15. Vogel P, Read RW, Hansen GM, Payne BJ, Small D, Sands AT, et al. Congenital hydrocephalus in genetically engineered mice. Vet Pathol. 2012; 49(1):166–81. [PubMed: 21746835]
16. Yang, P.; Smith, EF. The Flagellar Radial Spokes. In: Harris, EH., editor. The Chlamydomonas Sourcebook: Introduction to Chlamydomonas and Its Laboratory Use. Elsevier; 2009. p. 209-34.

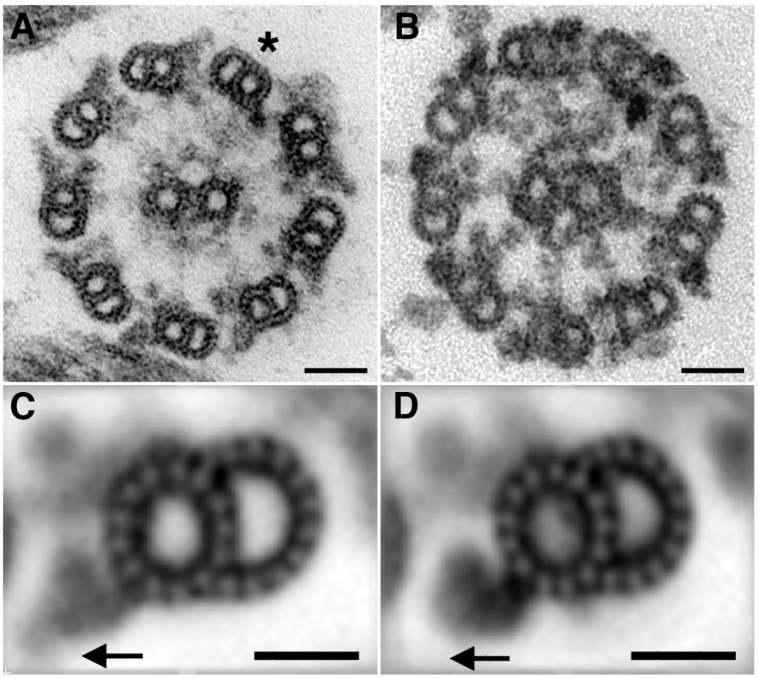

Figure 1. Axoneme cross sections from *Chlamydomonas* flagella and human cilia reveal similarities and differences.

(A) Typical cross section of a *Chlamydomonas* axoneme shows the typical 9 +2 arrangement of outer microtubule doublets surrounding a central pair complex. Doublet microtubules contain attached inner and outer dynein arms with doublet number one missing the outer arm (*). (B) Axonemes isolated from human respiratory cilia also contain the classic 9+2 arrangement of microtubules with all outer doublets containing an outer dynein arm. Central pair projections and radial spokes surround the central pair microtubules. (C) *Chlamydomonas* average containing 140 outer doublet cross sections. The outer dynein arm contains distinct lobes including an outer density (arrow). (D) Human ciliary average containing 110 doublets shows outer dynein arm density is reduced compared to *Chlamydomonas* (arrow). Bar = 50 nm A,B and 25 nm C,D.

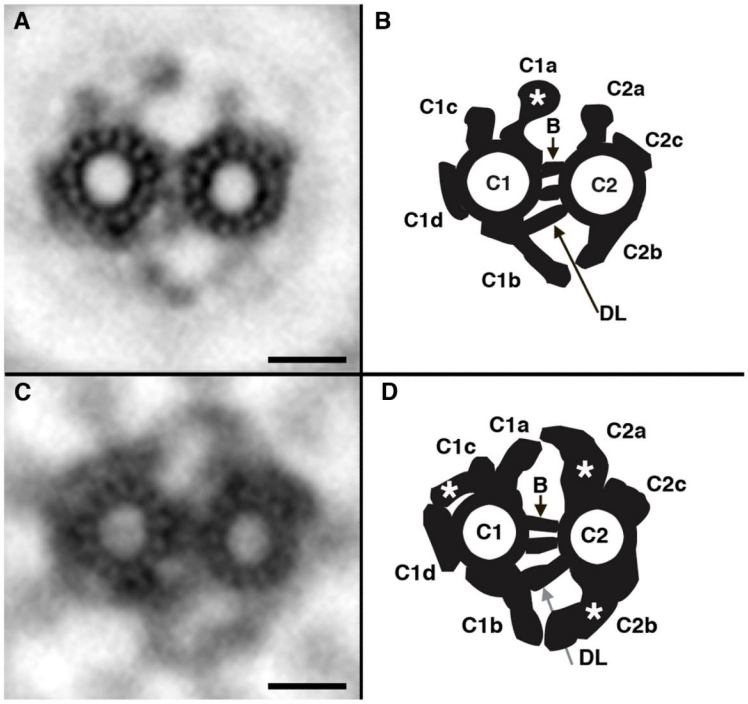

Figure 2. Central pair (CP) complex averages from *Chlamydomonas* and human cilia.

(A) *Chlamydomonas* average from 45 CP complexes. (B) Schematic of CP complex organization in *Chlamydomonas* based on the densities present in the *Chlamydomonas* average (modified from Lechtreck et al. 2008; Mitchell and Smith 2009). The CP microtubules (C1 and C2) are connected by a bipartite bridge (B) and diagonal linker (DL). CP projections extend out from the CP microtubules and the density of C1a is enhanced relative to human (*). (C) Human cilia average from 46 central pair complexes. Radial spokes are enhanced in the average. (D) Schematic of CP complex organization in human cilia based on the densities present in the human average. CP microtubules are connected by a bipartite bridge (B) and a diagonal linker (DL) is present. C1 and C2 projections are present. The density of the C2 projections is enhanced relative to Chlamydomonas (*). An additional density adjacent to C1c projection is present (*). Bar = 25 nm.

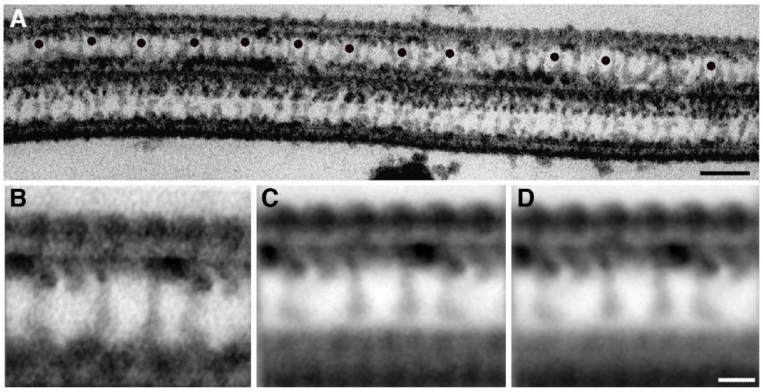

Figure 3. The complexity of inner arm organization is revealed in longitudinal averages from human cilia.

(A) Axonemes in longitudinal view are selected that contain two doublets separated by the central pair microtubules. The top doublet contains outer and inner dynein arms and radial spokes. Model points (black dots) show the center of the 96nm inner dynein arm repeat used for averaging. (B) Individual average containing the 12 repeats shown above. (C) Grand average from 13 axonemes and a total of 120 repeats. (D) Combined grand average from 2 people containing a total of 25 axonemes and 223 repeats. Bar = 100 nm (A); 25 nm (B-D)

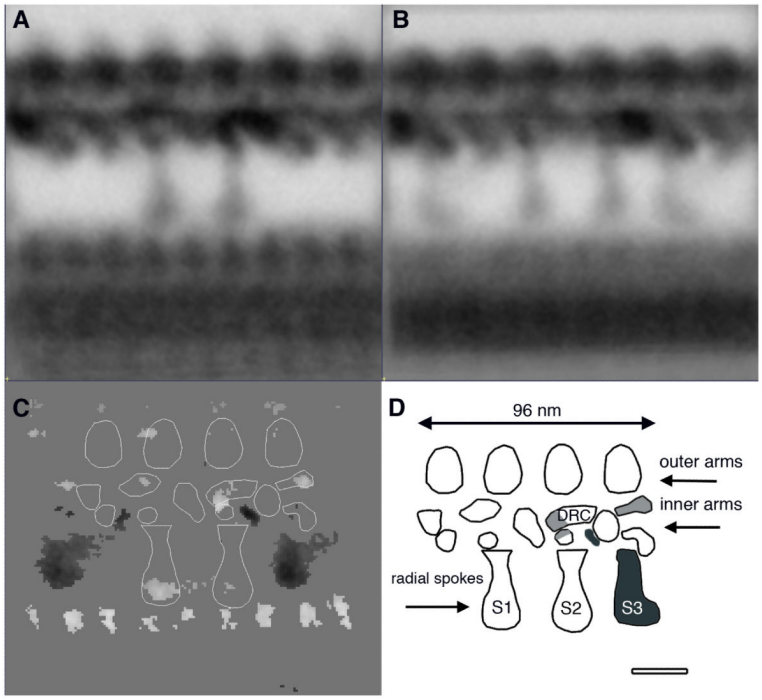

Figure 4. Analysis of axoneme longitudinal averages from *Chlamydomonas* flagella and human cilia.

(A) Averages from *Chlamydomonas* flagella based on a 96 nm repeating unit centered around 2 radial spokes. 2D averages resolve at least 10 densities in the inner dynein arm region. (B) Averages from human cilia show remarkable similarity in inner arm organization. Three radial spokes are present. (C) Diagram of densities within the *Chlamydomonas* 96 nm repeat and difference plots showing statistically significant differences between *Chlamydomonas* and human. Inner dynein arm organization is similar but human cilia have a reduced density corresponding to the dynein regulatory complex and a reduced density corresponding to a lobe distal the DRC. (D) Composite diagram showing inner arm organization along the 96 nm repeat with structures unique to *Chlamydomas* shaded in light gray and structures unique to human in dark gray (model modified from Porter and Sale 2000). Bar = 25 nm.

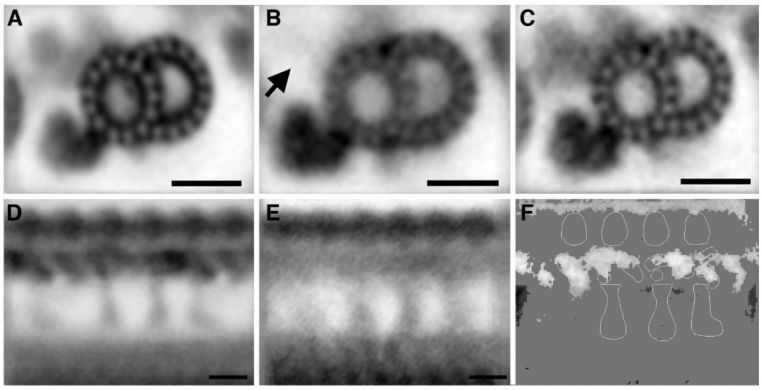

Figure 5. Image averaging is useful for analyzing defects in human ciliary axonemes.

(A) Average of 110 microtubule doublets imaged in cross section from axonemes of a normal individual. (B) An average of 132 doublet microtubules observed in cross-section from axonemes of a PCD patient. The density of the inner dynein arm is clearly reduced. (C) Average from a patient with cystic fibrosis (disease control, containing 109 doublets) shows dynein organization similar to the average from the normal individual. (D) Average of longitudinal sections from normal axonemes (25 axonemes/ 223 repeats) and (E) average of longitudinal sections obtained from the PCD patient (8 axonemes/ 65 repeats. (F) Difference image between normal and PCD axonemes shows the reduced inner dynein arm density in the axonemes from the PCD patient.

Table 1
Central pair microtubule associated polypeptides

Compilation of central pair proteins identified in *Chlamydomonas*, their structural location, and the most likely human orthologue, based on a Blast search of NCBI. The expected value and the maximum identity are presented, along with references indicating a role in mammalian cilia or flagella. Table is modified and updated from Mitchell, 2009 (23).

Central Pair Structure	Polypeptides identified in *Chlamydomonas* (Accession number)	Best blast hit in *Homo sapiens* (Accession number)	Properties	References
Cl-microtubule				
	PF16 (AAC49169)	SPAG6 (NP_036575.10) 63% identity	Armadillo repeat	Dutcher et al., 1984,(1) Smith and Lefebvre, 1996; (2)Neilson et al., 1999, (3)
	PP1c(AAD38856.1)	PP1-gamma catalytic subunit (NP_002701.1) 83% identity	Phosphatase	Yang et al., 2000, (4), Han et al., 2007(5)
Cla projection	PF6 (AAK38270)	SPAG17 (NP_996879) 1e-11, 56% identity	Alanine-proline rich; ASH domain	Rupp et al., 2001; (6)Wargo et al., 2005;(7) Zhang et al., 2005(8)
	C1a-86 (AAZ31187) (FAP101)	Weak homology to Tcte1 (EAX04266.1)	PKA Rll-like LRR domain	Wargo et al., 2005
	C1a-34 (AAZ31186) (FAP119)	C16orf93 (AAH9249.1) 5e-18, 27% identity	Coiled-coil, dimerizes with C1a-32	Wargo et al., 2005
	C1a-32 (AAZ31185) (FAP114)	Same as above	Similar to C1a-34	Wargo et al., 2005
	C1a-18 (AAZ31184)	MORN repeat 2 (NP_001138922.1) 1e-14, 40% identity	MORN domains	Wargo et al., 2005
	Calmodulin (AAA33083)	Calmodulin (NP_001734.1) 3e-94, 89% identity	EF hand Ca++ binding protein	Wargo et al., 2005
Clb projection	CPC1 (AAT40992.1)	Sperm flagellar protein 2 /KPL2 (NP_079143.3) 3e-49, 29%?identity	CH, adenylate kinase domains	Zhang and Mitchell, 2004; (9) Mitchell et al., 2005 (10) Ostrowski et al, 1999,(11) Sironen et al, 2006 (12)
	C1b-350 (FAP42) (EDP00757.1)	GUK1 (NP_00849.1) 3e-34, 38% identity	Guanylate and adenylate kinase domains	Mitchell et al., 2005
	C1b-135 (FAP69) (EDP06190)	C7orf63 (AAI41835.1) 7e-40, 21% identity	Armadillo repeat	Mitchell et al., 2005
	HSP70 (P25840.2)	HSP70-1L (NP_005518.3) 0.0, 74% identity	Chaperone	Bloch and Johnson, 1995; (13)Mitchell et al., 2005
	Enolase (XP_001702971)	Enolase (NP_001966.1) 0.0, 68%	Glycolytic enzyme	Mitchell et al., 2005
C1c projection	unknown			
C1d projection	FAP221 (ADD85929.2)	Pcdp1 (EAW95222.1/Q4GOU5.2) 6e-58, 38%	CaM binding	DiPetrillo and Smith, 2010;(14)Lee et al., 2008(15)
	FAP74 (ADD85930.1)	EAW56139.1 2e-85, 30%		
	FAP46 (EDP06555.1)	C10orf93 (AAH44661.1) 3e-18, 28%	TTC40	

Central Pair Structure	**Polypeptides identified in *Chlamydomonas* (Accession number)**	**Best blast hit in *Homo sapiens* (Accession number)**	**Properties**	**References**
	FAP54 (EDP00642)	C12orf55 (XP_001718035.3) 1e-21, 30%		
C2-microtubule				
C2a projection	unknown			
C2b projection	Hydin (EDP09735)	Hydin (NP_116210.2) 0.0, 44% identity	ASH domains	Lechtreck & Witman, 2007; (16) Davy and Robinson, 2003 (17)
C2c projection	KLP1(P46870/EDP06592)	KIF9 (NP_878905) 2e-127,34% identity	Kinesin-like protein	Bernstein et al., 1994, (18)Yokoyama et al., 2004 (19)
C1-C2 bridge	PF20 (P93107/AAB41727))	SPAG16 (NP_078808.3) 2e-140, 39% identity	WD-protein	Smith and Lefebvre, 1997; (20) Pennarun et al., 2002(21), Zhang et al., 2007(22)
Diagonal link	unknown			

Cytoskeleton (Hoboken). Author manuscript; available in PMC 2013 August 01.

Table 2

Radial spoke proteins

Compilation of radial spoke proteins identified in *Chlamydomonas* and the most likely human orthologue. Conserved functional domains, along with references indicating a role in mammalian cilia or flagella, are presented. Table is modified from Yang and Smith, 2009 (16).

***Chlamydomonas* Name**	***Homo sapiens* Name**	**Domains**	***Chlamydomonas* Accession**	***Homo sapiens* Accession**	**References**
RSP1	RSPH1 (Meichroacidin/TSGA2)	MORN	ABC02025	NP_543136.1	Yang et al., 2006; (1)Shetty et al., 2007(2)
RSP2	DYDC2 *	DBY, GAF, CAM	AAQ92371	NP_115748.1	Yang et al., 2004(3)
RSP3	RSPH3 (RSHL2)	AKAP	P12759	NP_114130	Williams et al., 1989(4)
RSP4	RSPH4A RSPH6A (RSHL3, RSHL1)	Spoke head	Q01656	NP_001010892 NP_110412 XP_294004	Curry et al., 1992(5) Castleman et al., 2009(6)
RSP5		Aldo-keto reductase	ABC02018		Yang et al., 2006
RSP6	RSPH4A RSPH6A (RSHL1, RSHL3)	Spoke head	B44498	NP_001010892 NP_110412 XP_294004	Curry et al., 1992 Castleman et al., 2009
RSP7	CALML5 *	Rlla, EF-hands	ABC02026	NP_059118.2	Yang et al., 2006
RSP8	ARMC4 *	Armadillo	ABC02019	NP_060546.2	Yang et al., 2006
RSP9	RSPH9 (C6orf206)	Spoke head	ABC02020	NP_689945.2	Yang et al., 2006 Castleman et al., 2009
RSP10	RSPH1 RSPH10B (TSGA2)	MORN	ABC02021	NP_543136.1 AAH34495.2 NP_775836	Yang et al., 2006
RSP11	ROPN1L ASP	Rlla	ABC02022	NP_114122.2	Yang et al., 2006 Fiedler et al., 2012 (7)
RSP12	PPIL6	PPI	ABC02023	NP_775943	Yang et al., 2006
RSP14	RTDR1	Armadillo	ABC02024	NP 055248	Yang et al., 2006
RSP15 (FAP201)		LRR	XP_001694808.1		Yang et al., 2006; Merchant et al., 2007(8)

***Chlamydomonas* Name**	***Homo sapiens* Name**	**Domains**	***Chlamydomonas* Accession**	***Homo sapiens* Accession**	**References**
RSP16	DNAJB13 (TSARG6)	DNAJ chaperone	EDP05321	NP_705842 NP_006136	Yang et al., 2005(9) Guan et al., 2010(10)
RSP17		GAF	ABC02027		Yang et al., 2006
RSP19		Beta-tubulin	P04690	Many	Yang et al., 2006
1 RSP20		Calmodulin	AAA33083	Many	Yang et al., 2001(11)1
RSP22	DYNLL2	Dynein Light Chain	Q39580	NP_542408	King and Patel-King, 1995;(12) Yang et al., 2009 (13)
RSP23 (LC8)	NME5	NDK, DPY, IQ	AAS15573 AY452667	NP_003542	Patel-King et al. 2004(14) Vogel et al., 2012 (15)

RSP13, RSP18, RSP21 have been identified as spots on 2D gels, but a full-length sequence has not been described.

*Best match, but low scoring.